Process Integration and Optimisation for Sustainability

Incorporating deposit ageing into visualisation of crude oil preheat train fouling

E.M. Ishiyama, S.J. Pugh and D.I. Wilson*

Corresponding author:

D. Ian Wilson

Department of Chemical Engineering and Biotechnology

Philippa Fawcett Drive

Cambridge

CB3 0AS

United Kingdom

E-mail diw11@cam.ac.uk

Tel +44 1223 334 791

FAX +44 1223 334 796

Incorporating deposit ageing into visualisation of crude oil preheat train fouling

E.M. Ishiyama[1], S.J. Pugh[1] and D.I. Wilson[2]*

[1]*formerly* IHS Downstream Research, 133 Houndsditch, London, EC3A 7BX, UK

[2] Department of Chemical Engineering and Biotechnology, University of Cambridge, Philippa Fawcett Drive, Cambridge, CB3 0AS, UK

Abstract

Fouling is an acute problem in crude oil preheat train heat exchangers as it affects the thermal and hydraulic performance of individual units as well as the network. Ageing of fouling deposits complicates these interactions and effective tools for visualising these effects are needed. The modified temperature field plot construction, devised by Graham Polley and co-workers in 2002, allows the impact of fouling on pressure drop and heat duty across individual units and the preheat train to be presented in a systematic way. The simple deposit ageing model of Ishiyama *et al*. (2010) was incorporated into the analysis of a simple preheat train based on that presented by Panchal and Huang-Fu (2000) to calculate the impact of ageing on fouling dynamics and network performance. The modified temperature field plot is shown to be effective in communicating the impact of fouling and ageing, allowing a designer or operator to be able to interpret correctly what might otherwise be conflicting trends or unexpected behaviour.

Keywords

Ageing; fouling; network; pressure drop.

Highlights

- Ageing can switch the main impact of fouling from duty loss to pressure drop
- The modified temperature field plot is an effective way of presenting the thermal and hydraulic performance of the network
- The plot allows the designer or operator to understand fouling impacts and assess mitigation options

Introduction

Crude oil distillation is the backbone of any oil refinery. Distillation is an energy intensive process and recovery of thermal energy from distillation products to the crude oil feed in a preheat train network is essential for economic operation. Many crudes and crude blends, however, promote fouling in the network exchangers, reducing the amount of heat transferred and increasing pressure drops which can limit throughput (Polley *et al*., 2009). Since crude distillation units (CDUs) are required to run continuously for periods of up to several years, fouling is often countered through a series of fouling mitigation options such as the use of antifouling chemicals, periodic removal of individual exchangers for cleaning, etc. A list of fouling mitigation options used in crude preheat trains are discussed in Ishiyama *et al*. (2019).

Optimisation of cleaning schedules for CDU network exchangers has received considerable attention over the last ten years (e.g. Rodriguez and Smith (2007); Ishiyama *et al*. (2009a, 2009b); Liu *et al*. (2015); Diaby *et al*. (2015); Diaz-Bejarano et al., (2016)), building on the development of quantitative models for predicting the rate of fouling in different exchangers, as reviewed by Wilson *et al*. (2017).

Optimising cleaning operations reduces the impact of fouling on performance, but it represents a method for coping with fouling rather than reducing the likelihood of fouling occurring. Graham Polley was one of the first workers to recognise the opportunity that quantitative predictive fouling models, such as that by Ebert and Panchal (1997), offered in terms of designing CDU preheat trains and individual CDU exchangers to reduce the extent of fouling and even prevent it occurring in certain units. His first paper on the topic (Wilson *et al*., 2002) combined Ebert and Panchal's quantitative model for predicting the rate of crude oil fouling with the temperature field plot, a graphical construction illustrating the matching of process streams with the cold crude. The Ebert and Panchal model allowed operating conditions (surface temperature, crude flow velocity) which would give low fouling rates to be identified. These 'fouling thresholds' were added to the temperature field plot so that optimal use of available pressure drop could be identified, both in green field design and revamping of existing networks. This approach allowed the maximum feasible heat recovery for a CDU to be determined, i.e. with manageable amounts of fouling and cleaning (Polley *et al*., 2002a; Polley *et al*., 2005).

Polley and co-workers subsequently extended the field plot to incorporate considerations of the impact of fouling on pressure drop (Yeap *et al*., 2004) and therefore unit throughput. Maintaining throughput is usually critical to the operation of CDUs: losses in heat transfer performance can be accommodated by extra furnace duty, but large pressure drops can result in the crude partially vapourising in exchangers upstream of the furnace (or in some cases

upstream of the preflash for networks where preflash columns are employed) as its pressure decreases and bulk temperature increases (Ishiyama and Pugh, 2015). Using first order models, they linked the thermal and hydraulic effects of fouling: they considered shell-and-tube exchangers as this configuration is the most common type used on refineries. Depending on the operating philosophy of the refinery, crude (or the higher fouling stream) may be allocated on the tubeside to facilitate easier cleaning. However, it is acknowledged that this is not always the case.

In this paper we revisit the modified temperature field plot to incorporate some of the developments made since 2004, many of which were inspired by Graham Polley's insight into the practical implications of fouling on CDU design and operation. Graham was a strong advocate of visualisation tools: the modified temperature field plot allows the user to assess at a glance the impact of fouling on the thermo-hydraulic performance of an exchanger and a network, and thus represents an important way of communicating this to the operators of such networks as well as designers looking at revamping, retrofitting and creating networks. The particular focus is on deposit ageing, which can introduce unexpected dynamics into preheat train performance.

Other workers have developed higher order models and more complex simulation tools (e.g. Diaz-Bejerano et al., 2016) which capture the dynamics of fouling and its impact on preheat train performance in greater detail. Effective presentation of that information in a coherent form remains an issue, as with other complex calculations, and the modified temperature field plot remains, in the authors' opinion, a versatile tool for this. Moreover, it can be used to present the results from complex simulations.

Quantifying the impact of fouling – the modified temperature field plot (MTFP)

The thermal effect of fouling is often quantified in terms of the fouling resistance, R_f, defined as the difference between the overall heat transfer coefficient, U, and its value when clean, U_o:

$$R_f = \frac{1}{U} - \frac{1}{U_o} \quad [1]$$

This can be written as

$$U = \frac{U_o}{1 + R_f U_o} = \frac{U_o}{1 + Bi_f} \quad [2]$$

where Bi_f is the fouling Biot number. Fouling affects pressure drop by changing the roughness of the surface and by narrowing the flow channel, *i.e*. reducing the inner diameter of a tube in

the case of tubeside fouling. For the case of a single phase liquid operated at constant flow rate in the turbulent regime, the ratio of the pressure drop across a tube with inner diameter d_i and fouling layer of thickness δ to that of the clean tube, ΔP^*, is given by (Yeap *et al*., 2004)

$$\Delta P^* \approx \frac{1}{(1 - 2\delta/d_\mathrm{i})^5} \quad [3]$$

If the fouling layer is thin and uniform, it can be treated as a thin slab. Yeap *et al*. showed that this is likely to apply in cases of chronic fouling in CDUs, which is the subject of this work. The fouling resistance can be related to the deposit thickness via

$$R_\mathrm{f} = \frac{\delta}{\lambda_c} \quad [4]$$

where λ_c is the deposit thermal conductivity. Equation [3] can then relate the thermal and hydraulic effects of fouling, *viz*.

$$\Delta P^* \approx (1 - 2\lambda_c \mathrm{Bi}_\mathrm{f}/U_\mathrm{o} d_\mathrm{i})^{-5} \quad [5]$$

In this expression, U_o and d_i are set by the design and operation of the heat exchanger. The deposit thermal conductivity is a material parameter, which is subject to substantial uncertainty. Crude oil deposits vary in composition (oil, metal oxides, carbonaceous material; Derakshesh *et al*., 2013) and λ_c is expected to lie in the range 0.2 W m^{-1}K^{-1} < λ_c < 3 W m^{-1}K^{-1} (Wilson and Watkinson, 1997; Derakshesh *et al*., 2013; Ishiyama *et al*. 2019). The impact of this uncertainty is demonstrated in Figure 1, which shows the effect of thermal conductivity on the relationship between Bi_f (and heat transfer performance) and ΔP^* (and throughput) calculated for a simple countercurrent heat exchanger with U_o and d_i values typical of those employed on CDU units (Panchal and Huang-Fu, 2000; Yeap *et al*., 2004). The range of Bi_f and ΔP^* values extend beyond those likely to be acceptable in practice.

It can be seen that as the thermal conductivity of the deposit increases, the relationship between the thermal and hydraulic effects change. Eqn. [4] shows that a deposit with a high thermal conductivity has a smaller effect on heat transfer. This has implications for preheat train operation, because whereas a loss in heat recovery can be countered by an increase in furnace duty (until a firing limit is reached), increasing pressure drop will eventually result in a reduction in throughput or flashing of the crude which is not so easily compensated for.

Equation [5] allows hydraulic considerations to be included alongside thermal ones in the modified temperature field plot (MTFP) and a brief explanation of the MTFP is given here. Figure 2 shows a schematic MTFP, where the abscissa is the crude oil bulk temperature, T_b. The crude-side heat transfer surface temperature, T_s, or film temperature, T_f, is plotted on the primary ordinate axis, depending on which is the key parameter affecting deposition. An

exchanger is then plotted as a line linking the values at the crude inlet and outlet. T_b also serves as a measure of heat duty as the crude is usually liquid throughout the train and its specific heat does not vary strongly with temperature.

The surface temperature, T_s, is often a key variable in quantitative models for calculating the fouling rate. The original work by Polley and colleagues considered the 'threshold fouling' model of Ebert and Panchal (1997), where the rate of change of fouling resistance (the 'fouling rate') on the crude-side was expressed in terms of a competition between a growth term and a suppression term, *viz*.

$$\frac{dR_f}{dt} = k_f\, v^m exp\left(-\frac{E_f}{RT_s}\right) - b\tau_w \qquad [6]$$

where t is time, v the bulk mean velocity, R the gas constant and k_f, b, E_f and m are model parameters. τ_w is the shear stress exerted by the flowing crude on the heat transfer (and subsequently the deposit) surface. The RHS of Equation [6] suggests that the fouling rate will be small or zero for some combination of T_s, T_b and v (as τ_w is determined primarily by v). This is the 'threshold fouling' concept introduced by Ebert and Panchal. It should be noted that negative fouling rates are not valid (shear driven removal of a mature CDU deposit is seldom observed in practice). On the MTFP loci are calculated for a set value of the fouling rate, *i.e*. zero or a value unlikely to give rise to significant change in performance over the desired operating period, as shown on Figure 2 where $v_1 < v_2 < v_3$. This allows the designer to identify matches which would cross one of the loci and therefore set the lowest allowable tubeside velocity to use in that unit.

Graham Polley published several papers on kinetic models for describing crude oil fouling (e.g. Polley *et al*., 2002b, Polley *et al*., 2007). Given the lack of laboratory experimental data, owing to the cost and complexity of conducting such experiments, he worked on different approaches to dealing with plant data, with a noteworthy emphasis on generating forms that could be used in practice for design or operation of units. His work on utilising fouling prediction models to predict performances of crude preheat trains and furnaces has been presented elsewhere (Ishiyama *et al*., 2012a, 2012b, 2011; Kumana *et al*., 2010; Morales-Fuentes *et al*., 2011; Polley *et al*., (2013, 2011b, 2011a)). The case study presented here employs the asphaltene precipitation model (APM) which he proposed (see Ishiyama *et al*. (2013)), where

$$\frac{dR_f}{dt} = \frac{k_{f,APM}}{h}\, exp\left(-\frac{E_f}{RT_f}\right)\left(1 - \left(\frac{\tau_w - 2}{c}\right)^{\frac{1}{2}}\right) \qquad \tau_w \geq 2 \text{ Pa} \quad [7a]$$

$$\frac{dR_f}{dt} = \frac{k_{f,APM}}{h}\, exp\left(-\frac{E_f}{RT_f}\right) \qquad \tau_w < 2 \text{ Pa} \quad [7b]$$

Here h is the film heat transfer coefficient for the crude stream, T_f is the film temperature and $k_{f,APM}$ is a constant specific to the crude. c is set at 98 Pa based on field experience. The form of the APM was developed for shell and tube devices: application to other geometries (*e.g*. compact heat exchangers) has yet to be established.

The APM does not predict a zero fouling rate so a threshold fouling rate needs to be specified, which is a design parameter. Here we use a fouling rate based on the uncertainty in U measurements based on plant data, and the timescale of the operation, *e.g*. the duration between shut-downs, t_{op}. A typical uncertainty (Mohanty, 2012) is 10%, which yields the following criterion from Equation [2]

$$\left(\frac{dR_f}{dt}\right)_{threshold} = \frac{\Delta R_f}{\Delta t} = \frac{1}{9U_o}\frac{1}{t_{op}} \quad [8]$$

with U_o being the clean heat transfer coefficient either for each exchanger, or for one at the hot end of the preheat train where fouling is expected to be fast (from Equation [7]).

The above construction occupies the upper diagonal of the TFP. In the modified TFP, the lower quadrant is used to present the hydraulic performance of the exchanger. Given its geometry and v, the tubeside pressure drop can be estimated. This is plotted as a box in the lower diagonal, with pressure drop as the secondary ordinate and T_b as before. The boxes form a set of steps and identify where the allowable pressure drop is allocated. Moreover, when fouling is not zero, the impact of fouling on the tubeside pressure drop can be estimated from Equation [5] and the box replotted. Exchangers which lie above the threshold for their tubeside velocity (or shear stress) will see an increase in the overall pressure drop over time. Similarly, the change in U as a result of fouling can result in a reduction in the heat duty, so the length of the box changes. These points are illustrated in Figure 2.

The calculations linking thermal and hydraulic performance require the timescale, t_{op}, which is a design variable, and the deposit thermal conductivity. Data on fouling deposit thermal conductivities are sparse and Table 1 summarises those which the authors have found from a search of the literature. It can be seen that there is considerable variation in the values so there is a need for more measurements of this thermophysical property. The low value reported by Derakshesh *et al.* (2013) arises from the measurements being made with a heated wire operating at constant heat flux, which promoted vapourisation of the oil in the porous deposit matrix. Equation [4] indicates that this would increase the insulating nature of the deposit significantly. Vapourisation of the crude also gives rise to large pressure drops and this gives rise to an additional locus on the MTFP, which is the total pressure drop and temperature at which vapourisation would occur. A generic locus is plotted on Figure 2: the

relationship is determined by the composition of the crude and the hydraulic configuration (including the pump characteristic) of the preheat train.

Deposit ageing

One aspect of fouling behaviour which has not been considered in the temperature field plot construction to date is deposit ageing, where the thermal and mechanical properties of the foulant change over time. Ageing has been considered in detailed simulations (Diaz-Bejarano *et al.* (2016)). At the temperatures encountered at the heat transfer surface, the deposit is transformed from its original structure to one resembling coke. The effect on λ_c is shown by the experimental data for mixtures of wax and carbon black, representing two limiting cases, in Figure 3. This is usually accompanied by a change in mechanical strength, which affects the selection of cleaning method.

Ageing is therefore important for CDU preheat trains, where units can be operated for several years between maintenance or cleaning actions. Ageing changes the relationship between the thermal and hydraulic performance of the exchanger. Equation [2] shows that increasing λ_c will reduce R_f but not ΔP^*, so that the hydraulic impact cannot be reliably gauged from heat transfer measurements. In the worst case, vapourisation will occur as the total pressure drop rises while the crude temperature remains quite high. Studies reporting deposit ageing in CDUs have been reported by Ishiyama *et al*. (2019), while quantitative approaches for modelling ageing have been presented by Ishiyama *et al*. (2010) and Coletti *et al*. (2010) Experimental studies of ageing to date have focussed on crystallisation (Brahim *et al*., 2003) and food (Davies *et al*., 1997) applications.

Incorporating ageing into the MTFP requires a quantitative model and here we use the first model on the topic, presented by Ishiyama *et al*. (2010). This assumes a linear dependence of λ_c on an ageing parameter, the youth factor y, where $0 < y \leq 1$, viz

$$\lambda_c = \lambda_{c,\infty} + y\left(\lambda_{c,0} - \lambda_{c,\infty}\right) \quad [9]$$

with y initially set at 1. The change in y follows a first order kinetic law

$$\frac{dy}{dt} = -k_a y \exp\left(\frac{E_a}{RT_d}\right) \quad [10]$$

where k_a is a rate constant, T_d is the local temperature in the deposit, and the temperature sensitivity is given by E_a.

Figure 4 shows how ageing can affect the thermo-hydraulic response of an exchanger to fouling. With no ageing, the thermal impact is mirrored by a hydraulic impact, so that a reduction in heat transfer is accompanied by an increase in pressure drop (for constant flow

rate operation). Ageing changes this: in the case of slow ageing, the impact on heat transfer levels off while the hydraulic penalty continues to grow. With fast ageing (converting the layer into a high thermal conductivity coating) the hydraulic penalty dominates. This makes interpretation of fouling data challenging, particularly as pressure drops are not measured as widely as heat transfer rates. More research needs to be done on this topic, a point made regularly by Graham Polley in his interrogation of conference presenters about the absence of pressure drop data in their papers.

Ageing is incorporated in the MTFP here by calculating λ_c at t_{op} and adjusting the Bi_f and ΔP values accordingly. One could perform the calculations over a series of times and animate the MTFP to illustrate the dynamics: this could be readily incorporated in software tools.

Case study

Network calculation

The above concepts are demonstrated using a preheat train based on that presented by Panchal and Huangfu (2000) which has been used by several workers to illustrate fouling in CDUs. The network of 22 individual shells (Figure 5) is not complicated as each hot stream is contacted with the crude once: in many refineries a hot stream can be involved in several matches, introducing feedback into the network performance (*e.g*. Ishiyama *et al*., 2009). The heat exchangers are arranged in six groups: those in E2-E6 feature two sets in parallel, which allows one set to be cleaned while the network continues to operate. Scheduling of such cleaning operations is not considered in this study.

The individual exchanger geometries are summarised in Table 2. The stream inlet conditions (flow rates and temperatures) are taken from Panchal and Huangfu, except for some of the product stream temperatures which did not reflect those coming from a typical atmospheric column and have been replaced with more values which the authors consider to be more realistic (Table 3).

Fouling models

Different fouling models were used to define fouling in different sections of the network. Upstream of the desalter the exchangers were assumed to have constant fouling rates of 2×10^{-8} $m^2K\ W^{-1}hr^{-1}$ (E1) and 4×10^{-8} $m^2K\ W^{-1}hr^{-1}$ (E2). These differed from those in the Panchal and Huangfu paper. This level of fouling meant that the desalter inlet temperature could be maintained at the target temperature of 120°C over the three year period, without resorting to cleaning upstream (see Ishiyama *et al*., 2010b)

Downstream of the desalter the Asphaltene Precipitation Model (Equation [7]) was used to model the dynamic fouling behaviour of the units in E3-E6, with E_f set at 44.3 kJ mol^{-1}, a set at 50 h^{-1} (within the range reported in (Ishiyama *et al*., 2014)) and a critical wall shear stress of 2 Pa, as above. This gives the fouling threshold relationship in Figure 6, calculated for h = 1000 W m^{-2} K^{-1}, with negligible fouling taken as build-up less than 5 ×10^{-4} m^2 K W^{-1} over 2 years. The x-axis is plotted in terms of wall shear stress rather than velocity, as this is the process parameter that appears in Equation [7] (and h is linked to τ_w). τ_w can be calculated for each exchanger. The threshold temperatures are not high, so fouling is expected to occur throughout the network.

Figure 7 shows the MTFP calculated for the APM with the parameters given. The MTFP is constructed from the outputs of the calculation. Fouling threshold loci are plotted for shear stresses of 2 Pa and 20 Pa, spanning the tubeside shear stresses which arise in E3-E6. It should be noted that the loci appear as horizontal lines on the plot as the model is written in terms of the film temperature, and this is used on the left-hand y-coordinate. The units in the network are plotted as solid lines (thermal) and boxes (hydraulic) with the τ_w values alongside.

It can be seen that exchangers E3 to E6 all lie above the fouling threshold. Moreover, all these units have low τ_w values (< 5 Pa when clean), so will encounter significant fouling, particularly E6 (with combination of low τ_w and high T_f). The fouling mechanism for exchangers E1 and E2 are not described by the APM and they are not relevant for the threshold fouling discussion. The main contributors to the pressure drop are E1 (low fouling), E3 (appreciable fouling) and E5 (heavy fouling), so the hydraulic impact of fouling will manifest strongly in E5 and possibly E6. Ageing is driven by surface temperature, so is expected to be more significant in E6 than E5.

All these points can be derived from the MTFP, illustrating its value in understanding the likely impacts of fouling. Wilson *et al*. (2002) describe how the MTFP could be used subsequently to consider mitigation by retrofitting the network. We focus here on the impact of ageing.

Deposit ageing model

The calculation approach presented by Ishiyama *et al*. (2010a) was implemented, where the deposit is treated as a series of thin layers laid down at time t_i, initially with thermal conductivity $\lambda_{c,0}$, and which subsequently undergoes ageing determined on the local temperature, $T_{d,i}$. A schematic of the process is shown in Figure 8. A detailed account of the calculation is given in Ishiyama *et al*. (2010a).

In the results presented here, the conditions in the network are calculated at intervals of length Δt: the fouling and ageing rates are then revised, and the amount of fresh deposit laid down over the interval added to each exchanger. The effective (overall) thermal conductivity of the deposit, λ_{eff}, is calculated from

$$\lambda_{eff} = \frac{\sum_{i=1}^{n} \delta_i}{\sum_{i=1}^{n} \frac{\delta_i}{\lambda_i}} \qquad [11]$$

δ_i is the thickness of deposit layer *i*, calculated from $\delta_{\text{i}} = \lambda_0 \frac{dR_{\text{f,i}}}{dt} \Delta t$, and *n* is the number of deposit layers deposited up to time t, given by $n(t) = t/\Delta t$. A Δt value of 1 week is used here.

Ageing rate constants

Given the lack of experimental data available, a series of scenarios is considered, similar to the approach reported by Ishiyama *et al*. (2010c). These differed in terms of initial rate (under initial operating conditions), labelled 'fast' and 'slow', and temperature sensitivity (high and low). The deposit thermal conductivity varies from 0.2 W $m^{-1}K^{-1}$ to 2.0 W $m^{-1}K^{-1}$. The sensitivity to temperature is quantified by E_a and two values are considered:

(i) 10 kJ mol^{-1}, which implies that to double the rate of reaction at the temperatures encountered at the hot end of this preheat train, the temperature would have to increase by approximately 200 °C. This means that the ageing rate will be effectively independent of fouling.

(ii) 200 kJ mol^{-1}, which implies high sensitivity to T_d: a roughly 5 °C increase in temperature would double the rate of reaction. The range of E_a from 10 to 200 kJ mol^{-1} is likely to cover the possible temperature kinetics experienced in a typical preheat train.

The scenarios are then

(i) Slow and low, with ageing rate constant $k_{a,slow,10}$ and E_a = 10 kJ mol^{-1}. The value used for $k_{a,slow,10}$ is 5×10^{-5} h^{-1}.

(ii) Fast and low, with $k_{a,fast,10} = 10\ k_{a,slow,10}$.

(iii) Slow and high, with $k_{a,slow,200} = k_{a,slow,10} \exp(22.85/T_s)$, compensating for the different temperature sensitivities.

(iv) Fast and high, with $k_{a,fast,200} = 10\ k_{a,slow,200}$.

The effect of ageing in exchanger E6B over the three year operating period is shown in Figures 9 and 10 for fast and slow ageing with two different temperature sensitivities, respectively. This unit features the highest crude and wall temperatures in the network and from the MTFP is expected to be subject to significant fouling. It is immediately upstream of the furnace so loss in heat transfer in E6B (and E6A) has a direct impact on network performance in terms of energy recovery. Figure 9(a) shows that fast ageing results in the effective thermal conductivity changing noticeably over time, even with a weak temperature dependency. There is little change in λ_{eff} for slow ageing. Figure 9(b) shows that fouling is significant in this unit (as expected from the MTFP): Bi_f reaches 6 and $\Delta P/\Delta P_{cl}$ exceeds 3 after 3 years in the absence of ageing. The slow ageing case shows significant thermal and hydraulic impacts ($Bi_f \rightarrow 4$, $\Delta P/\Delta P_{cl} \rightarrow 4$), with some recovery in heat transfer later on accompanied by increasing pressure drop.

Fast ageing results in Bi_f reaching a plateau value of ~ 1 early on, whilst $\Delta P/\Delta P_{cl}$ continues to increase. In this scenario the fouling dynamics would be masked in any monitoring based on thermal performance alone. This behaviour arises from the higher thermal conductivity of the deposit causing the surface temperature of the deposit to decrease less as a result of fouling, keeping the fouling rate high. A thicker fouling deposit is then generated, narrowing the flow path and increasing the pressure drop across the exchanger, by over 100%.

The fast ageing behaviour in Figure 9 is reproduced in Figure 10, where the increased temperature sensitivity of ageing drives a faster increase in λ_{eff}. Bi_f reaches a plateau value of approximately 0.5, representing a small impact on thermal performance, while $\Delta P/\Delta P_{cl} \rightarrow 6$ (slow ageing) and 8 (fast ageing). Such hydraulic losses are unlikely to be acceptable, and the simple hydraulic impact model is unlikely to be valid with a very thick deposit.

The corresponding plots for the other units in the network are provided in the Supplementary Information. These show similar trends to Figure 9, with smaller and slower changes as a result of the lower temperatures in these units.

Network performance

When clean, the crude entered the furnace at a temperature of 285°C and pressure of 23.5 bara. Figure 11 shows the furnace inlet temperature (FIT) and pressure (FIP) profiles over three year operation without cleaning. In the absence of ageing, the inlet temperature and pressure fall steadily to 217°C and 22 bara, respectively. The desalter temperature (not shown) stayed within its allowed range. Whilst the change in pressure is modest, the reduction

in FIT by nearly 70 K is unlikely to be acceptable and would require cleaning or a revamp of the network. In this regard, the MTFP becomes a useful tool because it indicates where the changes in thermal and hydraulic performance arise, and how the affected units relate to the fouling threshold.

Ageing improves heat transfer through the deposit (although it can also increase the amount deposited) and all the ageing scenarios result in a smaller change in FIT, and a greater reduction in FIP. In the fastest ageing scenario (fast ageing, E_a = 200 kJ mol^{-1}) FIT falls to 271°C and FIP to 20 bara. If monitoring temperature alone, it would not be possible to identify the hydraulic impact until an operational problem arose (such as the pumping capacity being reached and the crude boiling). The need for pressure drop measurements to help elucidate the actual performance of the network when subject to fouling and ageing is clear.

FIT and FIP constitute overall measures of the network performance. The impact of fouling and ageing within the network is conveniently presented in the MTFPs in Figure 12. The change in heat transfer is communicated by the change on the T_b scale while the change in pressure drop is marked by the height of the boxes and the τ_w values. Figure 12(a) shows the state after 3 years with no ageing. Comparing this with Figure 7, the change in FIT is evident, with only modest increases in T_b in E4, E5 and E6. The changes in pressure drop are across E5 and E6. Although the FIP is lower, the reduction in T_b in E6 may mean that vapourisation is avoided in this unit. However, the large reduction in FIT is likely to violate a furnace firing limit. Fouling mitigation measures are needed.

The impact of fouling on individual heat exchangers, and interactions between units, can be gauged from the change in size of the boxes in Figures 7 and 12. More detailed inspection can then be performed on the data used to construct the plots. The interactions can also be studied systematically using the network analysis techniques presented by Picón-Núñez and Polley (1995a,b).

Slow ageing (Figures 12 (b) and (c)) show smaller pressure drop increases in E5 and E6, accompanying increased duties in these units compared to the no ageing case. Comparing the MTFPs with that in Figure 7 again highlights where fouling, now with ageing, is causing the largest operating penalties. The MTFPs for the fast ageing scenarios (Figures 12(d) and (e)) show how large pressure drops arise in E5 and E6 with only small impacts on overall heat transfer, arising from the fouling rate staying high as a result of the deposit thermal conductivity quickly approaching that of a coke. The low absolute pressure in E6 is accompanied by a high T_b, which is likely to result in vapourisation. Moreover, the high pressure drop is likely to lead to reduced throughput as a result of the pump characteristics. This will have a direct impact on the production margin as preheat train operation economics are strongly affected by

throughput. Reduction in flow rate will also change the heat transfer characteristics (and surface temperatures) in the system, which the analysis would need to incorporate if these features were to be included. These are routinely calculated in modern CDU simulation tools.

These aspects of contrary thermo-hydraulic impacts arising from ageing were not considered by Polley and his co-workers when creating the MTFP. The Case Study demonstrates that the construction is able to visualise these quite effectively, so the designer or operator can see where fouling is likely to occur and how big an effect it will have on the network. Approaches for revamping and retrofitting preheat trains based on MTFPs have been presented in Yeap *et al*. (2003) and Wilson *et al*. (2005): the reader is referred to these earlier contributions from Graham Polley and co-workers rather than reproducing the material here.

Conclusions

Fouling is a chronic operating problem in the oil refining sector and is expected to continue to pose problems in future. Understanding the impact of fouling on the thermal and hydraulic performance of heat exchangers subject to fouling can be aided by the use of visualisation tools such as the modified temperature field plot introduced by Polley and co-workers. This construction has been modified here to include considerations of deposit ageing, using a simple ageing model in a case study based on a simple preheat train network. The shifting of the balance between thermal and hydraulic impacts of fouling caused by ageing are found to propagate into the network performance. The modified temperature field plot is shown to be an effective way to present the results of detailed analysis for the network designer or operator to gauge the contribution from the different factors involved. This demonstrates the need to monitor pressure drops in preheat trains subject to fouling, and to analyse the operating data carefully.

Acknowledgements

Many of the ideas presented here were birthed and refined during discussions between the authors and Dr Graham Polley.

Conflict of Interest

On behalf of all authors, the corresponding author states that there is no conflict of interest.

Nomenclature

Roman

b	exponent, Equation [6], $m^2K\ Pa^{-1}J^{-1}$
Bi_f	fouling Biot number, -
c	exponent, Equation [7], Pa
d_i	tube inner diameter, m
E_a	activation energy for ageing, J mol^{-1}
E_f	activation energy for deposition, kJ mol^{-1}
h	film heat transfer coefficient, W $m^{-2}K^{-1}$
k_a	ageing kinetic parameter, s^{-1}
k_f	deposition rate constant, $m^{2-m}K\ W^{-1}\ s^m$
$k_{f,APM}$	deposition rate constant, Equation [7], s^{-1}
m	exponent, Equation [6], -
n	number of deposit layers, -
ΔP	pressure drop, Pa
ΔP_{cl}	pressure drop when clean, Pa
ΔP^*	dimensionless pressure drop, -
R	gas constant, J $mol^{-1}\ K^{-1}$
R_f	fouling resistance, $m^2K\ W^{-1}$
t	time, s
t_{op}	operating interval, s
T	temperature, K
T_b	bulk temperature, K
T_{cold}	bulk crude temperature, K
T_d	deposit temperature, K
T_f	film temperature, K
T_s	surface temperature, K
U_o	overall heat transfer coefficient (clean), W $m^{-2}\ K^{-1}$
U	overall heat transfer coefficient, W $m^{-2}\ K^{-1}$
v	mean flow velocity, m s^{-1}
y	ageing variable (youth factor), -

Greek

δ	deposit thickness, m
λ_c	deposit thermal conductivity, W $m^{-1}\ K^{-1}$
$\lambda_{c,0}$	thermal conductivity, fresh deposit, W $m^{-1}\ K^{-1}$
λ_c	thermal conductivity, coked deposit, W $m^{-1}\ K^{-1}$
λ_{eff}	effective thermal conductivity, composite deposit, W $m^{-1}\ K^{-1}$
τ_w	wall shear stress, Pa

References

Brahim, F., Augustin, W. and Bohnet, M. (2003) Numerical simulation of the fouling process, Intl. J. Therm. Sci, 42(3), 33-334.

Brown, A.R.G., Watt, W., Powell, R.W., Tye, R.P., 1956. The thermal and electrical conductivities of deposited carbon. Br. J. Appl. Phys. 7, 73–76. https://doi.org/10.1088/0508-3443/7/2/309

Coletti, F., Ishiyama, E.M., Paterson, W.R., Wilson, D.I. and Macchietto, S. (2010) Impact of deposit ageing and surface roughness on thermal fouling: distributed model, AIChEJ*,* 56(12), 3257-3273.

Coletti, F., Macchietto, S. and Polley, G.T. (2011) Effects of fouling on performance of retrofitted heat exchanger networks: A thermo-hydraulic based analysis, Computers Chem. Eng., Vol. 35(5), 907 – 917.

Davies, T.J., Henstridge, S., Gillham, C.R. and Wilson, D.I. (1997) Investigation of milk fouling deposit properties using heat flux sensors, Food Bioproducts Processing, 75, 106-110

Derakshesh, M., Eaton, P., Newman, B., Hoff, A., Mitlin, D. and Gray, M.R. (2013) Effect of asphaltene stability on fouling at delayed coking process furnace conditions, Energy Fuels, 27 (4), 1856–1864.

Diaby, A.L., Miklavcic, S.J., Bari, S., Addai-Mensah, J., 2016, Evaluation of crude oil heat exchanger network fouling behavior under aging conditions for scheduled cleaning, Heat Transfer Engineering, 37(15), 1211-1230.

Diaz-Bejarano, E., Coletti, F., Macchietto, S. (2016) A new dynamic model of crude oil fouling deposits and its application to the simulation of fouling-cleaning cycles. AIChEJ. 62, 90–107.

Ebert, W. and Panchal, C.B.,(1997) Analysis of Exxon crude-oil slip stream coking data, in Fouling Mitigation of Industrial Heat Exchange Equipment, Panchal, C.B., Bott, T.R., Somerscales, E.F.C. and Toyama, S.. (eds.), Begell House, NY, 451-460.

Evans, A. (1968) Fouling characteristics of ASTM jet A fuel when heated to 700 deg F in a simulated heat exchanger tube. Technical report NASA TN D-4958. NASA.

Fan, Z, Watkinson A,P. (2006) Formation and characteristics of carbonaceous deposits from heavy hydrocarbon coking vapors. *Industrial and Engineering Chemistry Research*, 45(19), 6428–6435.

Fan, Z. (2006) Formation and characteristics of carbonaceous deposits from heavy hydrocarbon vapours. PhD Dissertation, University of British Columbia, Canada, https://doi.org/10.14288/1.0058724

Güralp, O. A., 2008. The effect of combustion chamber deposits on heat transfer and combustion in a homogeneous charge compression ignition engine (PhD Thesis). University of Michigan, Michigan, USA.

Ishiyama, E.M., Paterson, W.R. and Wilson, D.I. (2009) A platform for techno-economic analysis of fouling mitigation options in refinery preheat trains, Energy & Fuels, 23 (3), 1323-1337 schedules, Heat Transfer Engineering, 30(10-11), 805-814.

Ishiyama, E.M., Coletti, F., Machietto, S., Paterson, W.R. and Wilson, D.I. (2010a) Impact of deposit ageing on thermal fouling, AIChEJ, 56(2), 531–545.

Ishiyama, E.M., Heins, A.V., Paterson, W.R. Spinelli, L. and Wilson, D.I. (2010b) Scheduling cleaning in a crude oil preheat train subject to fouling: incorporating desalter control, Applied Thermal Eng., 30, 1852-1862.

Ishiyama, E.M., Paterson, W.R. and Wilson, D.I. (2010c) Exploration of alternative models for the ageing of fouling deposits, (2010) AIChEJ, 57(11), 3199-3209.

Ishiyama, E.M., Pugh, S.J., Wilson, D.I., Paterson, W.R., Polley, G.T. (2011) Importance of data reconciliation on improving performances of crude refinery preheat trains, in Proc. AIChE Annual Meeting, Conference Proceedings. Presented at the 7th Global Congress on AIChE Process Safety conference, Chicago.

Ishiyama, E.M., Polley, G.T., Pugh, S.J. (2012a) Recent experiences on modelling fouling of crude refinery preheat trains handling complex and heavy crude slates, in Proc. AIChE Annual Meeting.

Ishiyama, E.M., Pugh, S.J., Polley, G.T., Wilson, D.I. (2012b) Industrial experience in handling cleaning of crude refinery preheat trains, in proc. AIChE Annual Meeting.

Ishiyama, E.M., Pugh, S.J., Kennedy, J., D.I. Wilson, D.I., Ogden-Quin, A. and G. Birch, G. (2013) An industrial case study on retrofitting heat exchangers and revamping preheat trains subject to fouling, Proc. Intl. Conf. Heat Exchanger Fouling and Cleaning, http://heatexchanger-fouling.com/papers/papers2013/05_Pugh_F.pdf.

Ishiyama, E.M., Paterson, W.R. and Wilson, D.I. (2014a) Ageing is important: closing the fouling-cleaning loop, Heat Transfer Engineering, 35(3), 311-326.

Ishiyama, E., Kennedy, J., Pugh, S.J. (2014b). Scopes for improvements on preheat trains of crude refineries subject to fouling. Presented at the 17th Topical on Refinery Processing 2014 - Topical Conference at the 2014 AIChE Spring Meeting and 10th Global Congress on Process Safety, pp. 492–505.

Ishiyama, E.M., Falkeman, E.S, Wilson, D.I. and S.J. Pugh, S.J. (2020) Quantifying implications of deposit aging from crude refinery preheat train data, Heat Transfer Engineering, 41(2), 138-148 .

Kern, D.Q. (1957) Process Heat Transfer, McGraw-Hill, NY.

Kumana, J.D., Polley, G.T., Pugh, S.J., Ishiyama, E.M. (2010) Improved energy efficiency in CDUs through fouling control, in Proc. AICHE Spring Meeting. San Antonio, Texas, Paper No. 99a

Liu, L.-L., Fan, J., Chen, P.-P., Du, J., 2015, Synthesis of heat exchanger networks considering fouling, aging, and cleaning, Industrial and Engineering Chemistry Research, 54(1), 296-306.

Maksimovskii, V.V., Raud, É.A., Sokolov, O.A., Korsak, I.V., Chepovskii, M.A., 1990. Thermal conductivity of coke deposited in quenching-evaporative equipment of pyrolysis units. Chemistry and Technology of Fuels and Oils 26, 584–587.

Mayhew, E., Prakash, V., (2013) Thermal conductivity of individual carbon nanofibers. Carbon 62, 493–500. https://doi.org/10.1016/j.carbon.2013.06.048

Mohanty, D.K. (2012) Estimation and Prediction of Fouling Behaviour in a Shell and Tube Heat Exchanger. PhD thesis, Birla Institute of Technology and Science, Pilani (Rajasthan), India .

Morales-Fuentes, A., Rodriguez, G.M., Polley, G.T., Picon-Nunez, M., Ishiyama, E.M., (2011) Simplified analysis of influence of preheat train performance and fired heater design on fuel efficiency of fired heaters. Proc. 9th International Conference on Heat Exchanger Fouling and Cleaning, Crete, Greece.

Nelson, W. L. (1939) Fouling of heat exchangers. Refiner & Natural Gasoline Manufacturer, 13, (7), 271-276.

Panchal, C.B. and Huang-Fu, E.P. (2000) Effects of mitigating fouling on the energy efficiency of crude–oil distillation, *Heat Transfer Eng.*, 21, 3-9.

Perry, R.H., Green, D.W. (2007) Perry's chemical engineers' handbook. McGraw-Hill.

Picón-Núñez, M. and Polley, G.T. (1995a) Determination of the steady-state response of heat-exchanger networks without simulation, *Chem. Eng. Res. Des*., 73, 49-58.

Picón-Núñez, M. and Polley, G.T. (1995b) Applying basic understanding of heat exchanger network behaviour to the problem of plant flexibility, *Chem. Eng. Res. Des*., 73, 941-952.

Polley, G.T., Wilson, D.I., Yeap, B.L. and Pugh, S.J. (2002a), Use of crude oil threshold data in heat exchanger design, Applied Thermal Engineering, 22, 763-776.

Polley, G.T., Wilson, D.I., Yeap, B.L. and Pugh, S.J. (2002b), Evaluation of laboratory crude oil fouling data for application to refinery pre-heat trains, Applied Thermal Engineering, 22, 777-788.

Polley, G.T., Wilson, D.I., Petitjean, E. and Derouin, C. (2005) The fouling limit in crude oil pre-heat train design, Hydrocarbon Processing, July, 71-80.

Polley, G.T., Wilson, D.I., Pugh, S.J. and Petitjean, E. (2007) Extraction of crude oil fouling model parameters from plant exchanger monitoring, Heat Transfer Eng., 28(3), 185-192.

Polley, G.T., Tamakloe, E., Ishiyama, E., Pugh, S.J. (2011a) Analysis of plant data, in Proc. 11AIChE - 2011 AIChE Spring Meeting and 7th Global Congress on Process Safety.

Polley, G.T., Wilson, D.I., Ishiyama, E. (2011b) Mitigation of fouling in pre-heat trains, in: Proc. AIChE - 2011 AIChE Spring Meeting and 7th Global Congress on Process Safety, Chicago.

Polley, G.T., Tamakloe, E., Picon Nunez, M., Ishiyama, E.M., Wilson, D.I. (2013) Applying thermo-hydraulic simulation and heat exchanger analysis to the retrofit of heat recovery systems. Appl. Therm. Eng. 51, 137–143.

Robinson, A.L., Buckley, S.G., Baxter, L.L., (2001) Experimental measurements of the thermal conductivity of ash deposits: Part 1. Measurement technique, Energy Fuels, 15, 66–74. https://doi.org/10.1021/ef000036c

Rodriguez, C. and Smith, R., 2007, Optimization of operating conditions for mitigating fouling in heat exchanger networks, Chem. Eng. Res. Des., 85(6), 839 – 851.

Watkinson, A.P. (1988) Critical Review of Organic Fluid Fouling: Final Repot, ANL/CNSV-TM-208, Argonne National Laboratory, I11.

Watkinson, A.P. and Wilson, D.I. (1997) Chemical reaction fouling: A review, Exptl Therm. Fluid Sci., Vol. 14, 361 – 374.

Wang, Y., and Smith, R. (2013) Retrofit of a heat-exchanger network by considering heat-transfer enhancement and fouling. Ind. Eng. Chem. Res., 52, 8527–8537.

Weidenlener, A., Pfeil, J., Kubach, H., Koch, T., Forooghi, P., Frohnapfel, B., Magagnato, F., (2018) The influence of operating conditions on combustion chamber deposit surface structure, deposit thickness and thermal properties. Automot. Engine Technol. 3, 111–127. https://doi.org/10.1007/s41104-018-0030-3

Wilson, D.I., Polley, G.T. and Pugh, S.J. (2002) Mitigation of crude oil preheat train fouling by design, Heat Transfer Engineering, 23, 24-37.

Wilson, D.I., Polley, G.T. and Pugh, S.J. (2005) Ten years of Ebert-Panchal and the 'threshold fouling' concept, in *Proc*. 6th International Conference on Heat Exchanger Fouling and Cleaning - Challenges and Opportunities, Kloster Irsee, Germany.

Wilson, D.I., Ishiyama, E.M., Paterson, W.R. and Watkinson, A.P. (2009) Ageing: looking back and looking forward, *Proc*. Intl. Heat Exchanger Fouling Cleaning VIII, http://www.heatexchanger-fouling.com/papers/papers2009/32_Wilson_%20Ageing_F.pdf

Wilson, D.I., Ishiyama, E.M. and Polley, G.T. (2017) Twenty years of Ebert and Panchal – what next?, Heat Transfer Engineering, 38(7-8), 669-680.

Yeap, B.L.,Wilson, D.I., Polley, G.T. and Pugh, S.J. (2003) Retrofitting crude oil refinery heat exchanger networks to minimise fouling while maximising heat recovery, in Proc. 5th International Conference on Heat Exchanger Fouling and Cleaning: Fundamentals and Application, Santa Fe, New Mexico, USA.

Yeap, B.L., Wilson, D.I., Polley, G.T. and Pugh, S.J. (2004) Mitigation of crude oil refinery heat exchanger fouling through retrofits based on thermo-hydraulic fouling models, Chem. Eng. Res. Des., 82A, 53-71. [Erratum 84A, 248]

Table 1: Thermal conductivity of carbonaceous fouling deposits. Values reported are at 15 ^{o}C, unless otherwise stated.

Deposit	Thermal conductivity W m^{-1} K^{-1}	Source
Delayed coking furnace deposit	0.03	Derakshesh *et al.* (2013)
Coke flakes	0.07 – 0.15	Nelson (1939)
Ash deposits	0.11 to 0.17	Robinson *et al.* (2001)
Jet fuel foulant deposit	0.12	Evans (1968)
Crude preheat train deposits based on pressure drop data	0.1 to 1	Ishiyama *et al*. (2018)
Combustion chamber deposits	0.17 to 0.8	Weidenlener *et al*. (2018)
Combustion chamber deposits	1.5	Güralp (2008)
Coke-like deposit	0.5 – 1	Watkinson (1988)
Amorphous to condensed coke	0.55 to 76	Fan (2006)
Coke deposit (from pyrolysis unit)	1 – 4	Maksimovskii *et al*. (1990)
Graphite powder	1.8	Perry and Green (2007)
Carbon nano fibres	3 to 10	Mayhew and Prakash (2013)
Petroleum coke	5.8 (at 100 ^{o}C)	Kern (1957)
Carbon deposited at 2100 °C	5.6 (at 50 °C) 4.9 (at 200 °C)	Brown *et al*. (1956)
at 2000 °C	4.6 (at 50 °C) 4.2 (at 200 °C)	
at 1900 °C	0.89 (at 50 °C) 0.97 (at 200 °C)	
at 1800 °C	0.27 (at 50 °C) 0.32 (at 200 °C)	
Commercial graphite	0.89 (at 50 °C) 0.89 (at 200 °C)	

Table 2: Case Study heat exchanger tube-side geometries (per shell). The shell-side exchanger geometries were not reported. Fixed heat transfer coefficients, which differ from those in Panchal and Huang-Fu (2000), were used on the shell-side.

	E1	E2	E3	E4	E5	E6
Number of tubes per shell	916	1256	907	911	1288	1464
Tube internal diameter (cm)	2.11	2.11	2.11	2.11	2.11	2.11
Number of tube-side passes	4*	4**	4**	4**	4**	4**
Internal heat transfer area (m^2)	208	1152	208	523	1478	1344
Shell-side heat transfer coefficient (W $m^{-2}K^{-1}$)	1000	2510	300	300	300	300
Flow area (m^2)	0.160	0.220	0.159	0.159	0.225	0.256

* this exchanger had 1 tube-pass in the original paper.

** these exchangers had 2 tube-passes in the original paper

Table 3: Case Study stream inlet conditions

Stream	Flow rate	Inlet temperature	
		Panchal and Huangfu (2000)	(This work)
	kg s^{-1}	°C	°C
Crude	136	20	20
TPA	265	336	170
Kerosene	15.2	226	226
LGO	36	299	280
HGO	108	371	310
BPA	104	299	320
Residue	68	374	340

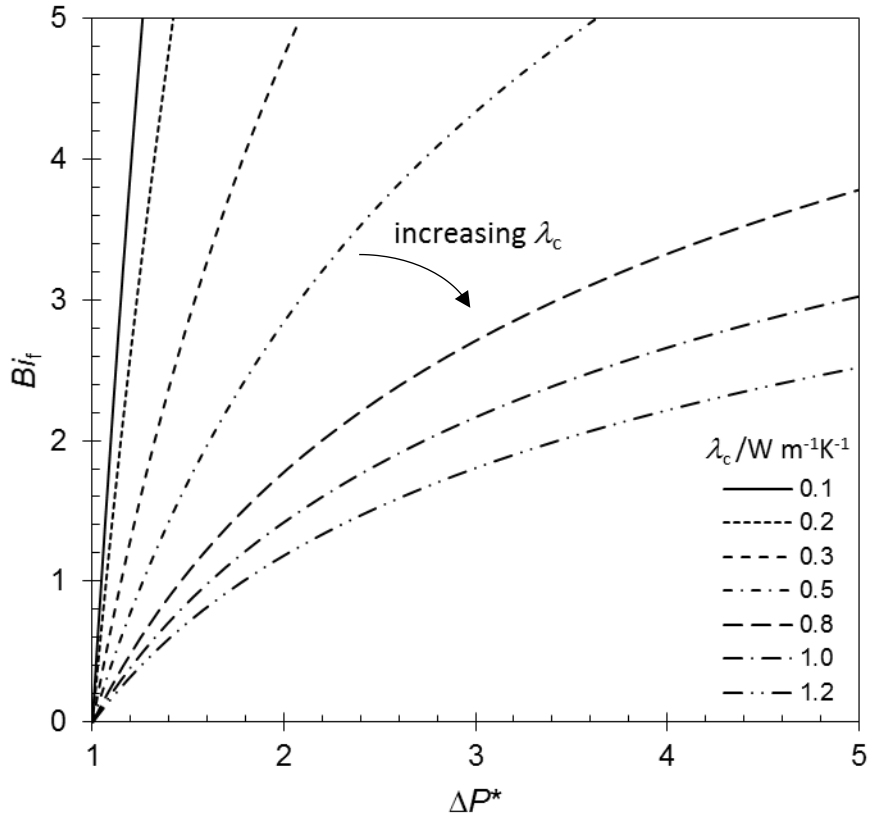

Figure 1 – Effect of deposit thermal conductivity on thermo-hydraulic performance of simple counter-current heat exchanger. Equation [5] plotted for the case where U_o = 1000 Wm^{-2}K^{-1}, d_i = 22 mm.

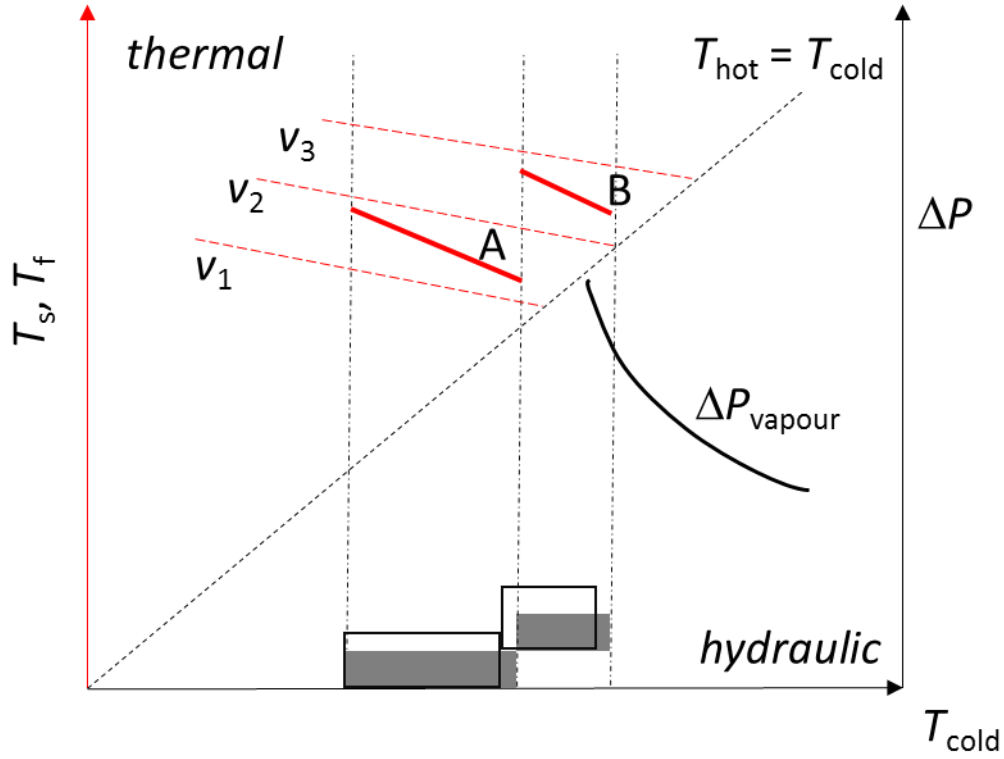

Figure 2 Schematic of modified temperature field plot. Upper quadrant: dashed lines labelled v_i show fouling threshold for velocity v. Solid lines indicate heat exchanger matches. Lower quadrant: bold line shows vapourisation threshold. Grey boxes indicate clean pressure drop, open boxes pressure drop across a fouled exchanger after a given operating time, *e.g.* t_{op}.

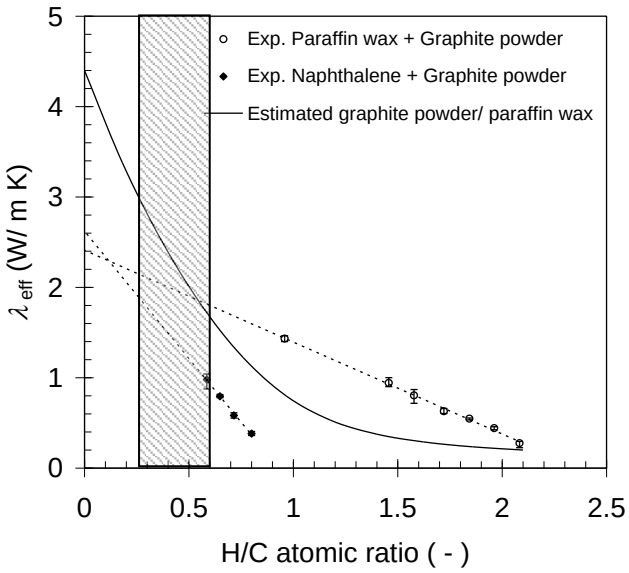

Figure 3 Effective thermal conductivity estimated for graphite powder/paraffin wax mixtures (solid line) and experimental measurements of mixtures of graphite powder and naphthalene (solid symbols) and paraffin wax (open symbols), after Wilson *et al*. (2009). The shaded region indicates the range of H/C ratios reported by Fan and Watkinson (2008).

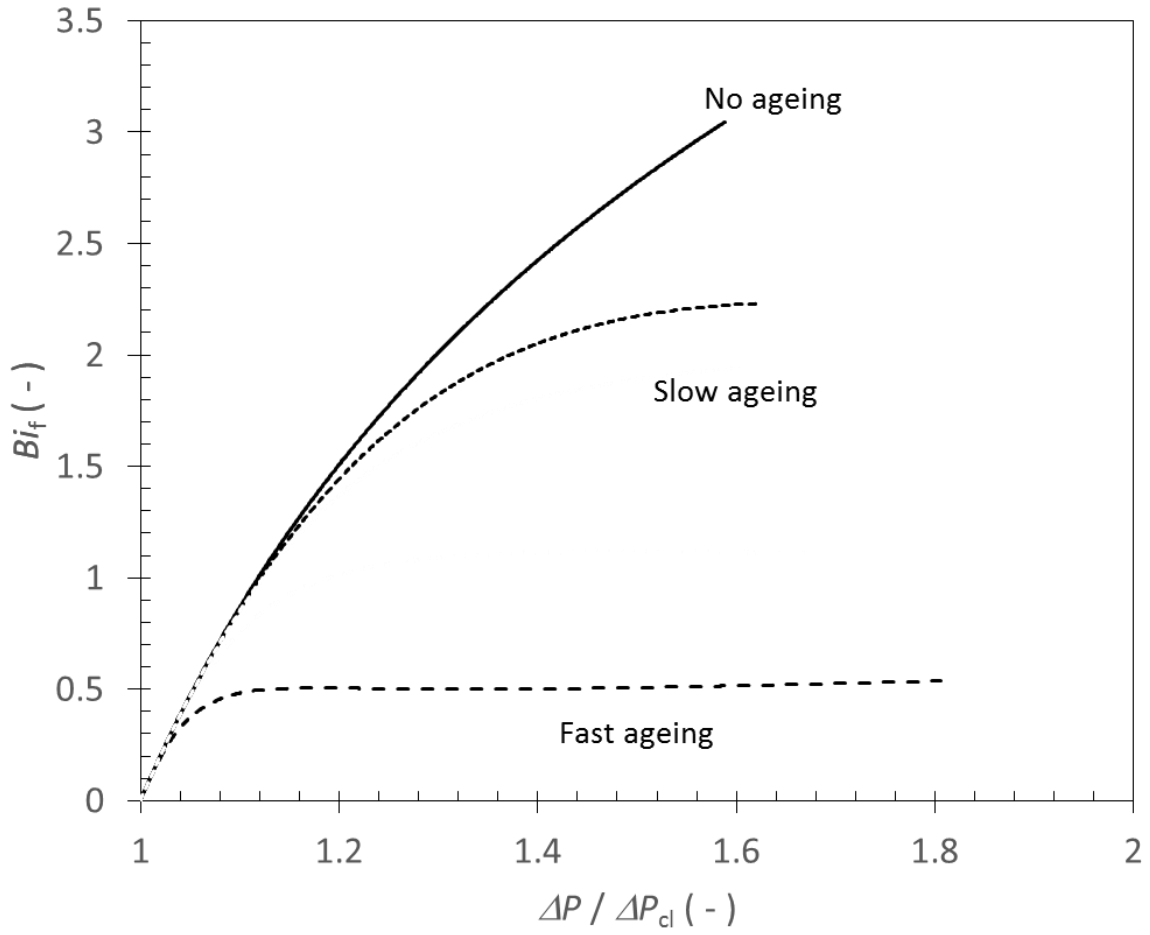

Figure 4. Thermo-hydraulic impact of fouling for an exchanger subject to severe fouling (Equation [5]) with (i) no ageing – constant thermal conductivity, λ_c = 0.2 W $m^{-1}K^{-1}$; (ii) slow ageing; and (iii) fast ageing, both with λ_c changing from 0.2 W $m^{-1}K^{-1}$ to 2.0 W $m^{-1}K^{-1}$.

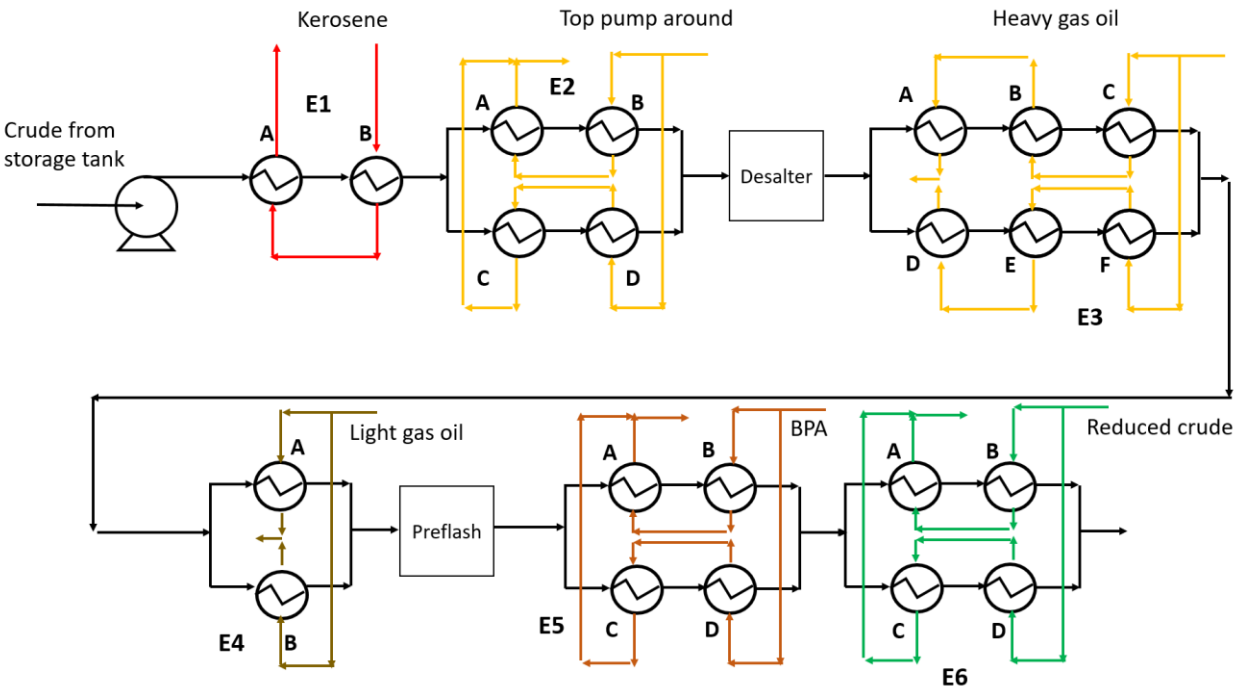

Figure 5: Case Study preheat train model based on Panchal and Huang-Fu (2000). Label Ei indicates a group of exchangers, with individual units labelled A, B, etc. Exchanger parameters, flow rates, temperatures are given in Tables 2 and 3.

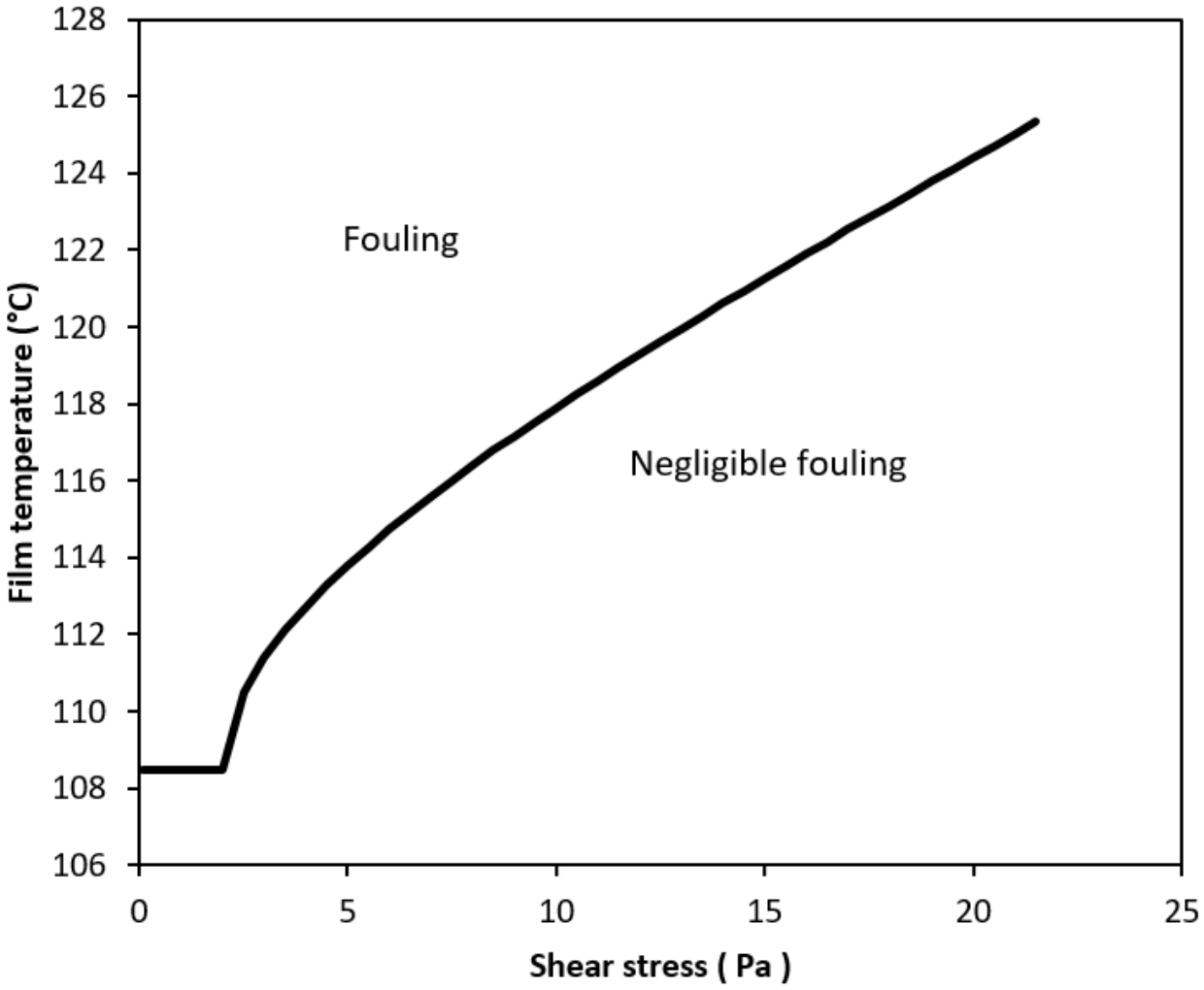

Figure 6 Fouling threshold plot calculated for APM (Equation [7],with h = 1500 W m^{-2} K^{-1}, a = 50 h^{-1}). Threshold given by Equation [8], where 'no fouling' corresponds to $R_f < 5\times10^{-4}$ m^2 K W^{-1} after 2 years of operation.

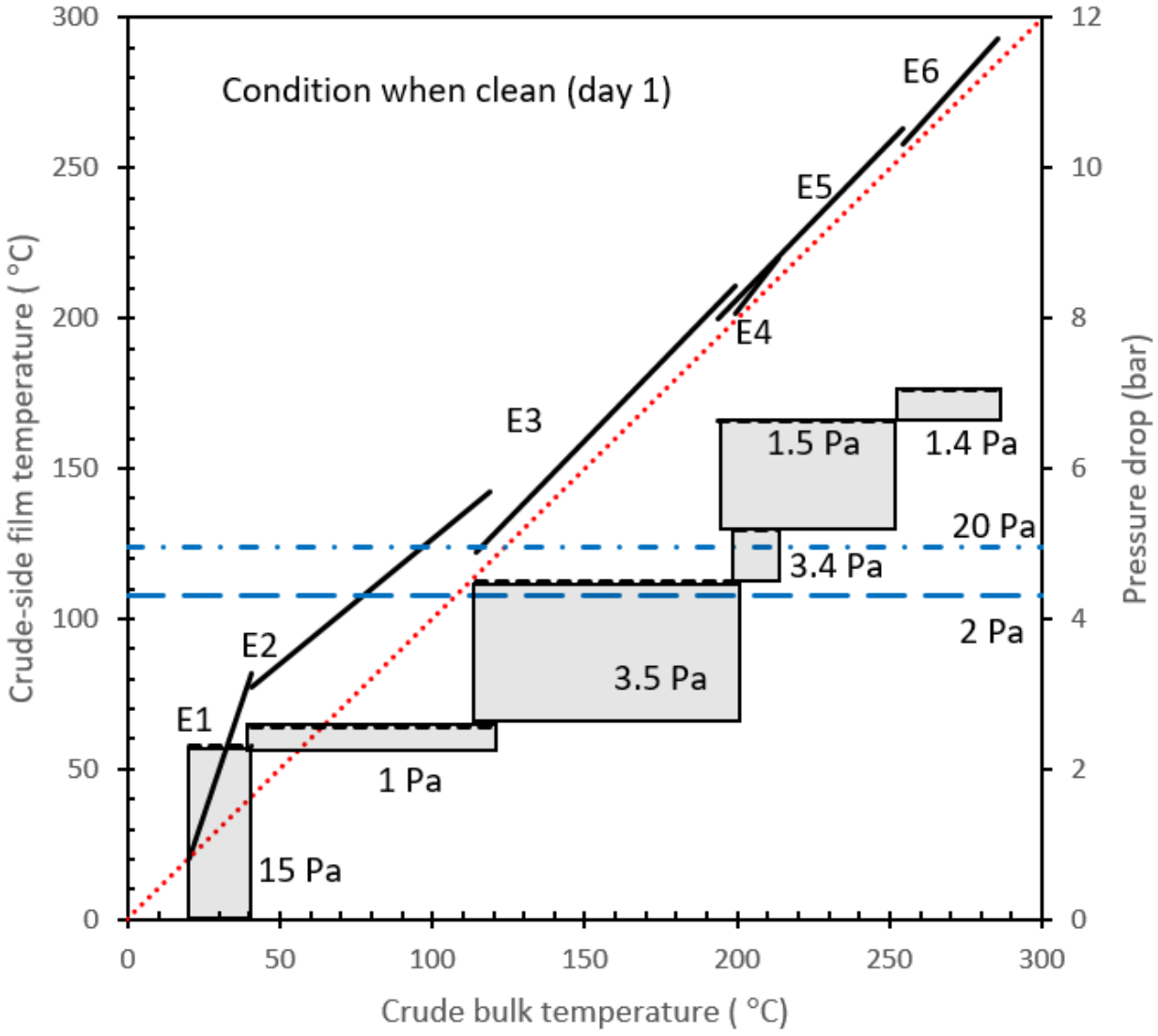

Figure 7. Modified temperature field plot for the Case Study network when clean. Diagonal dashed line is the line of equality, *i.e.* $T_f = T_b$. Exchangers are plotted as solid lines (thermal performance) and boxes (pressure drop), the latter labelled with the average tubeside shear stress. Horizontal dashed lines show the fouling threshold condition.

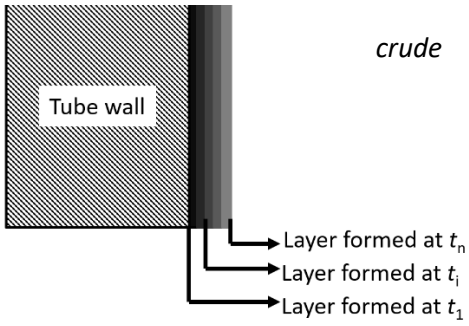

Figure 8: Deposit ageing: schematic of deposit layers with different ages formed on the tube wall. t_i denotes the i^{th} time step.

(a)

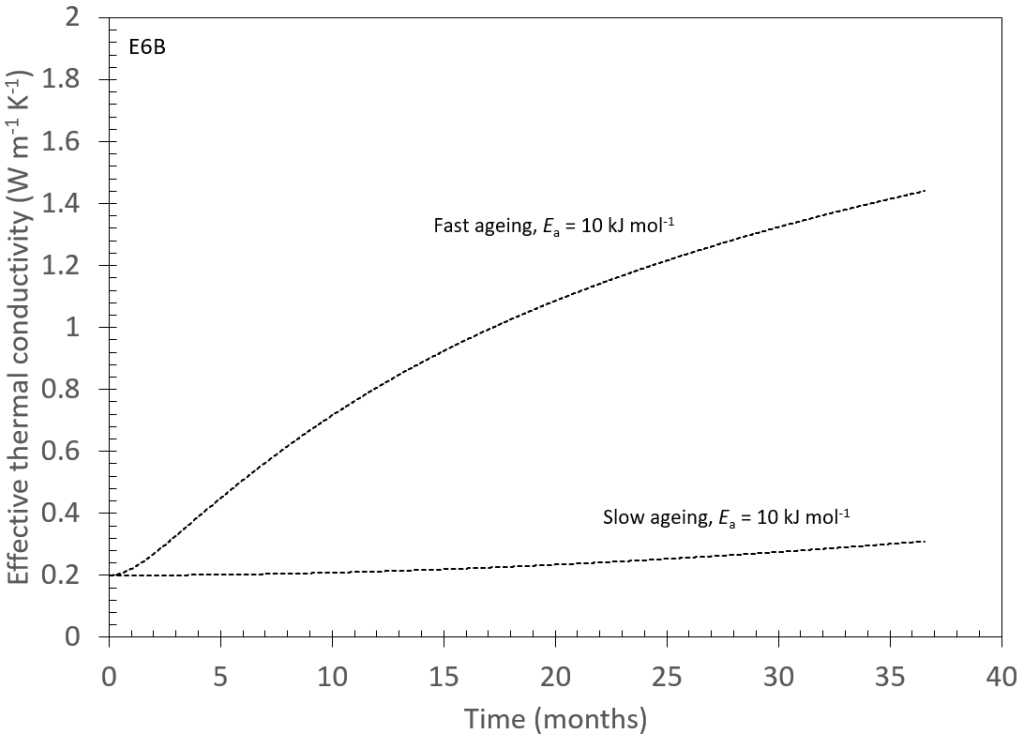

(b)

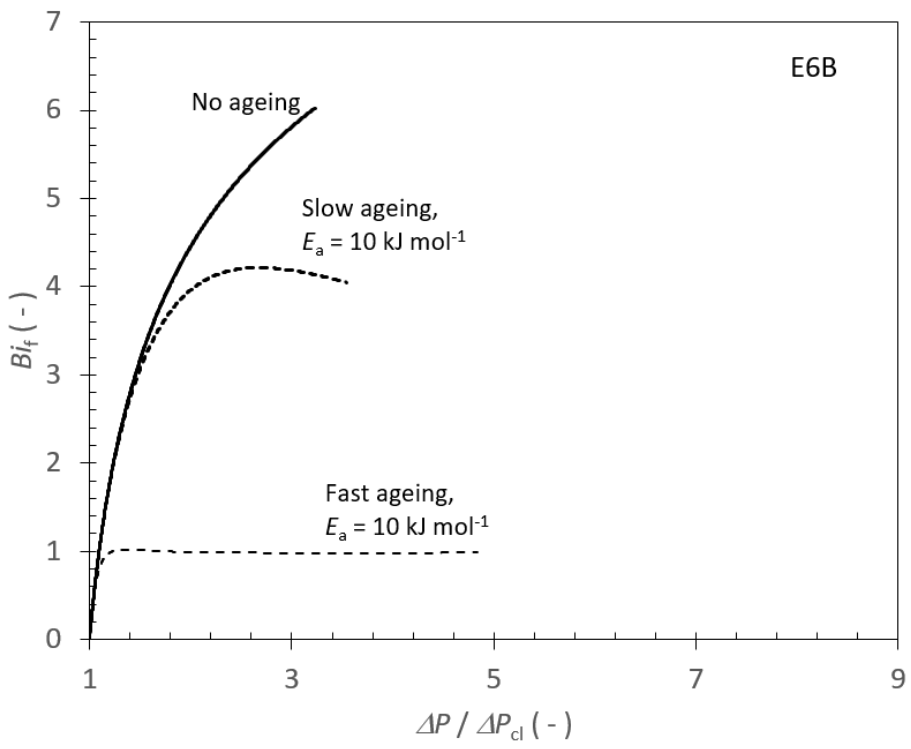

Figure 9: Evolution of (a) effective deposit thermal conductivity and (b) thermo-hydraulic performance in Case Study exchanger E6B for fast and slow ageing with weak temperature dependency.

(a)

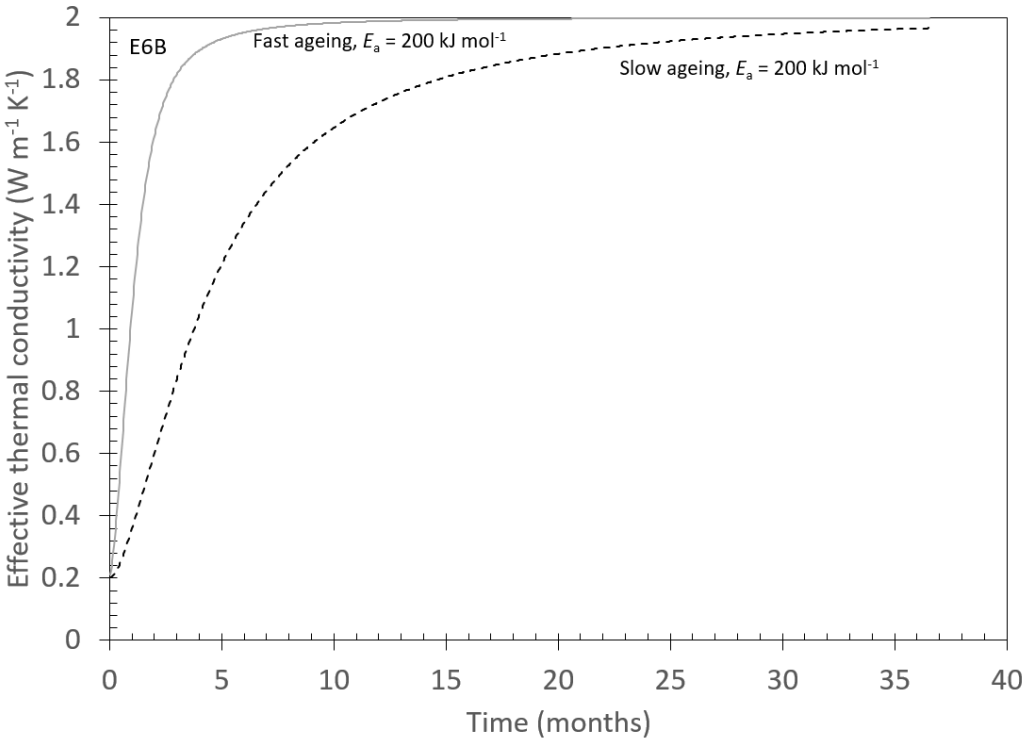

(b)

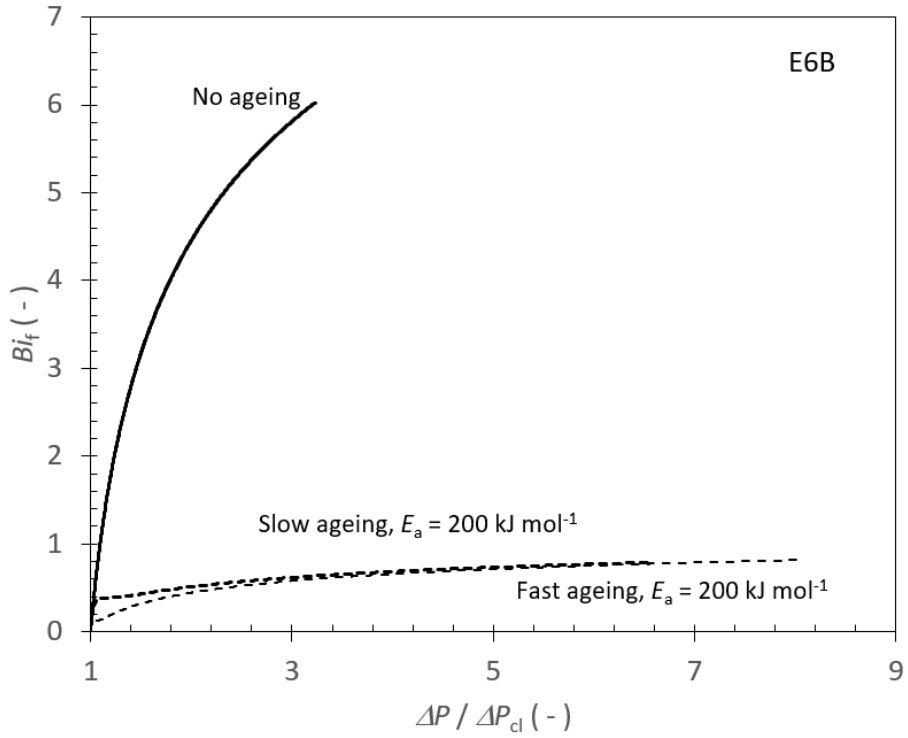

Figure 10: Evolution of (a) effective deposit thermal conductivity and (b) thermo-hydraulic performance in Case Study exchanger E6B for fast and slow ageing with strong temperature dependency.

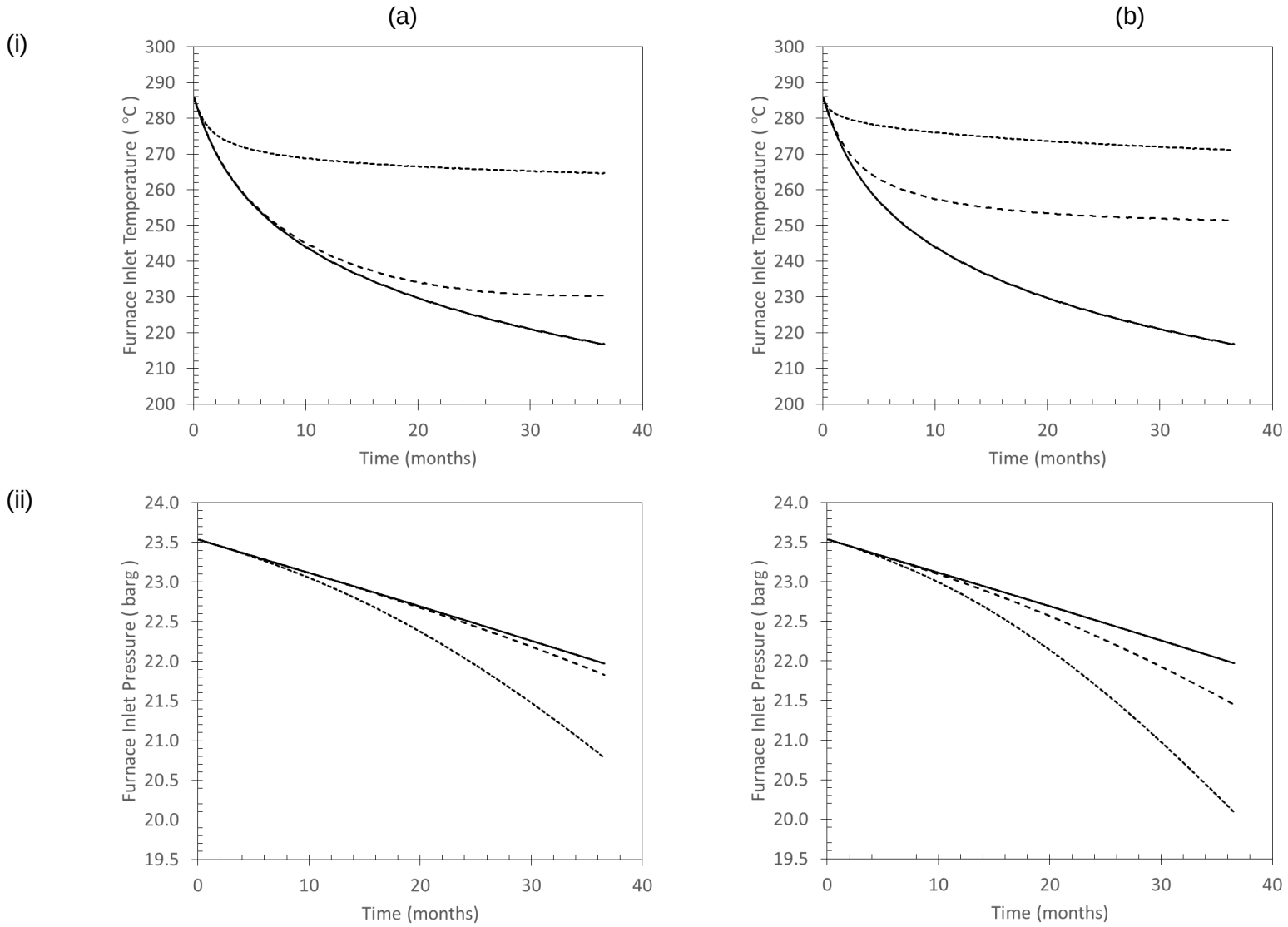

Figure 11 Combined effect of fouling and ageing on network performance, quantified by furnace inlet (i) temperature and (ii) pressure. Solid line – no ageing; dashed line – slow ageing; dotted line- fast ageing, for (a) weak temperature dependency and (b) strong temperature dependency.

(a)

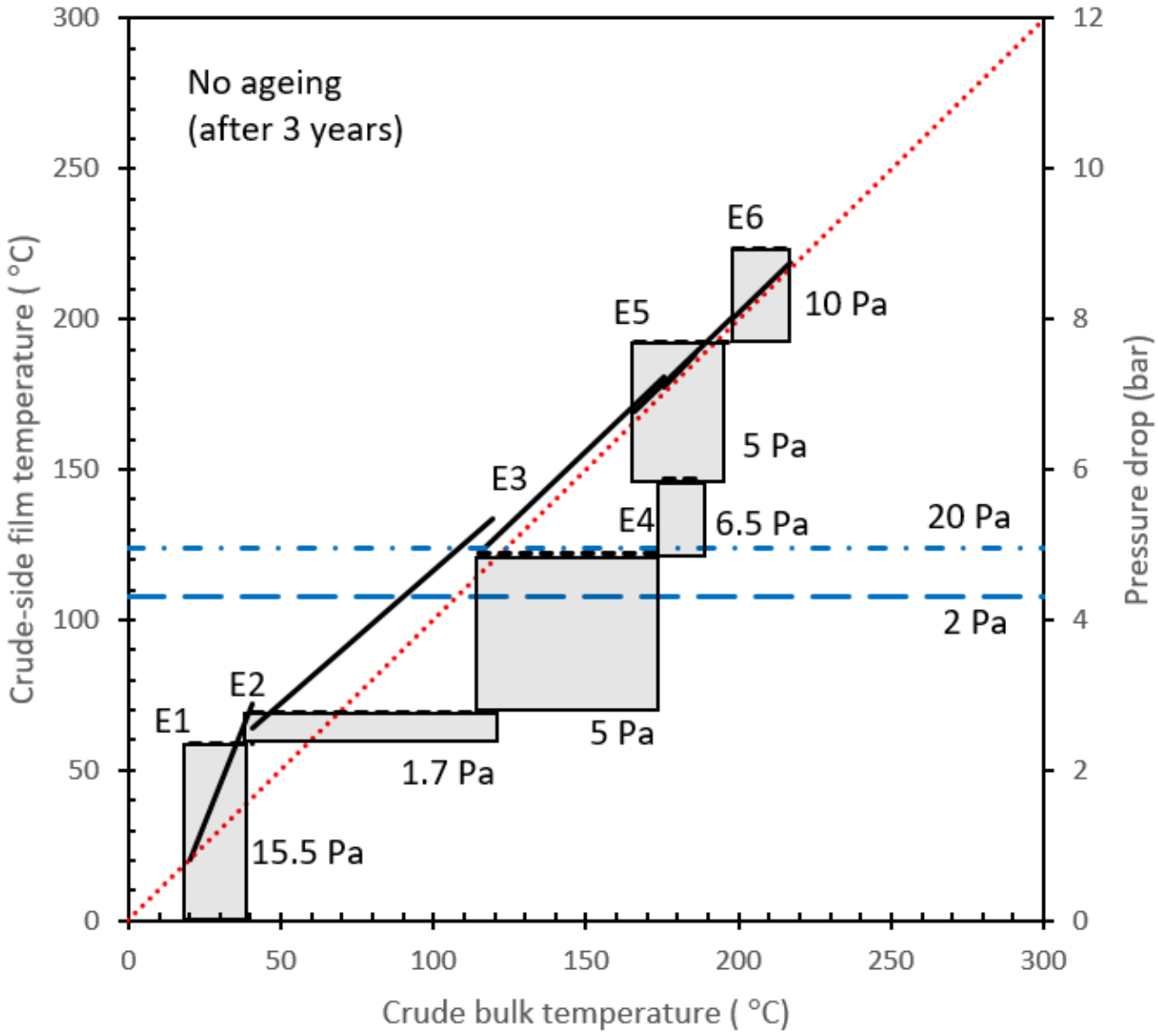

Figure 12. Modified temperature field plot for the Case Study network when after three years with (a) no ageing; (b) slow ageing, weak temperature dependency; (c) slow ageing, strong temperature dependency; (d) fast ageing, weak temperature dependency; (e) fast ageing, strong temperature dependency.

(b)

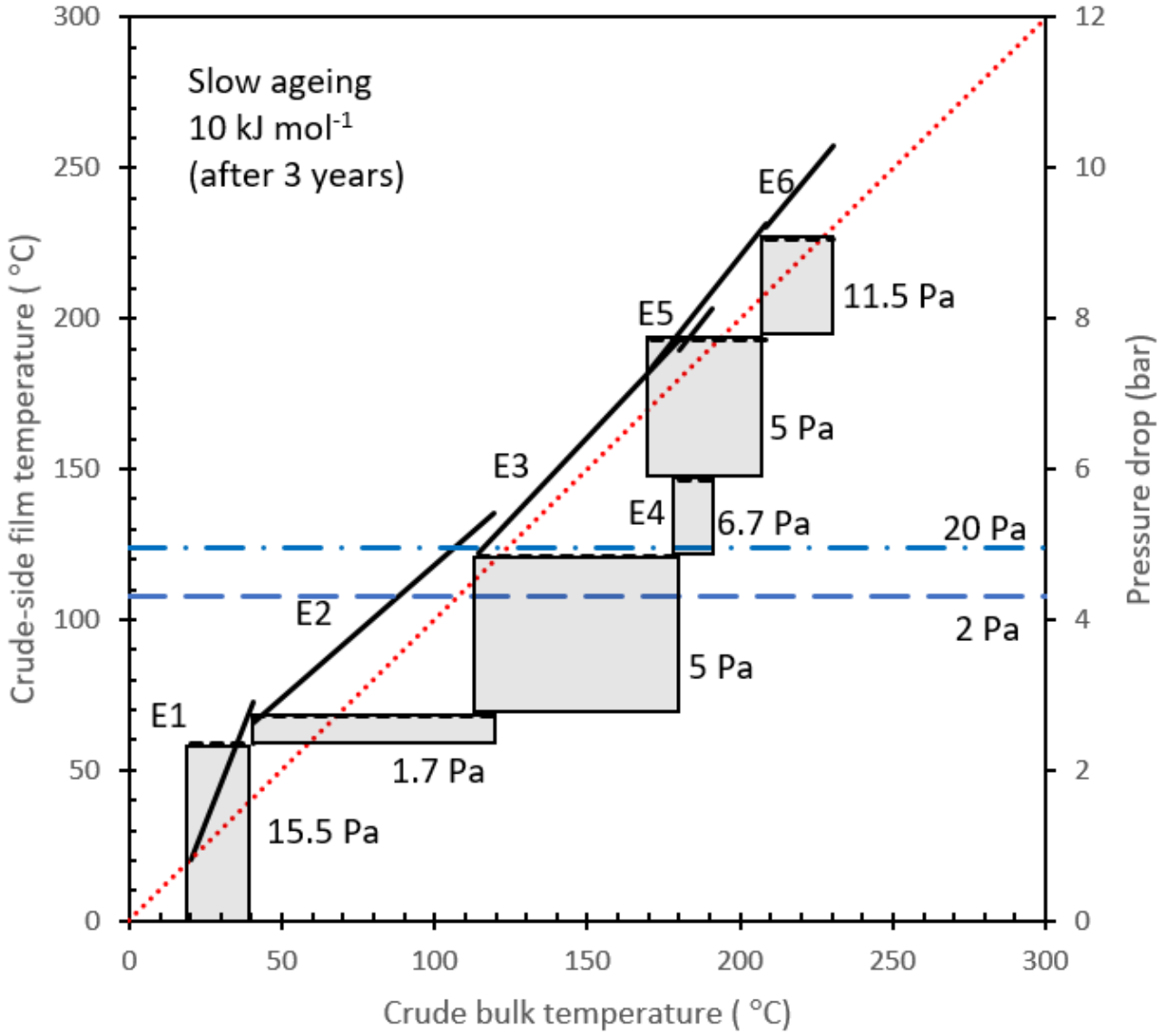

Figure 12. Modified temperature field plot for the Case Study network when after three years with (a) no ageing; (b) slow ageing, weak temperature dependency; (c) slow ageing, strong temperature dependency; (d) fast ageing, weak temperature dependency; (e) fast ageing, strong temperature dependency.

(c)

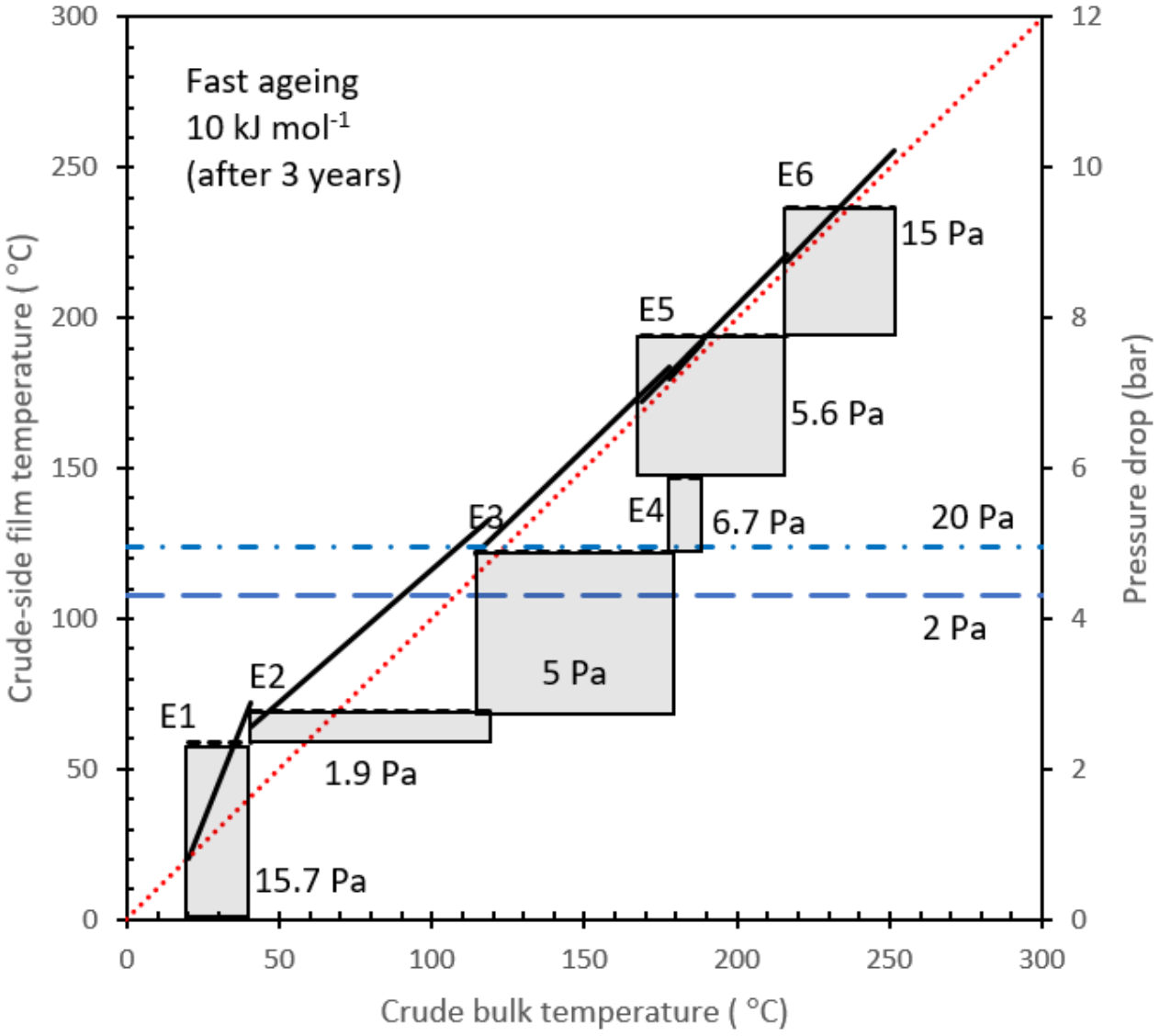

Figure 12. Modified temperature field plot for the Case Study network when after three years with (a) no ageing; (b) slow ageing, weak temperature dependency; (c) slow ageing, strong temperature dependency; (d) fast ageing, weak temperature dependency; (e) fast ageing, strong temperature dependency.

(d)

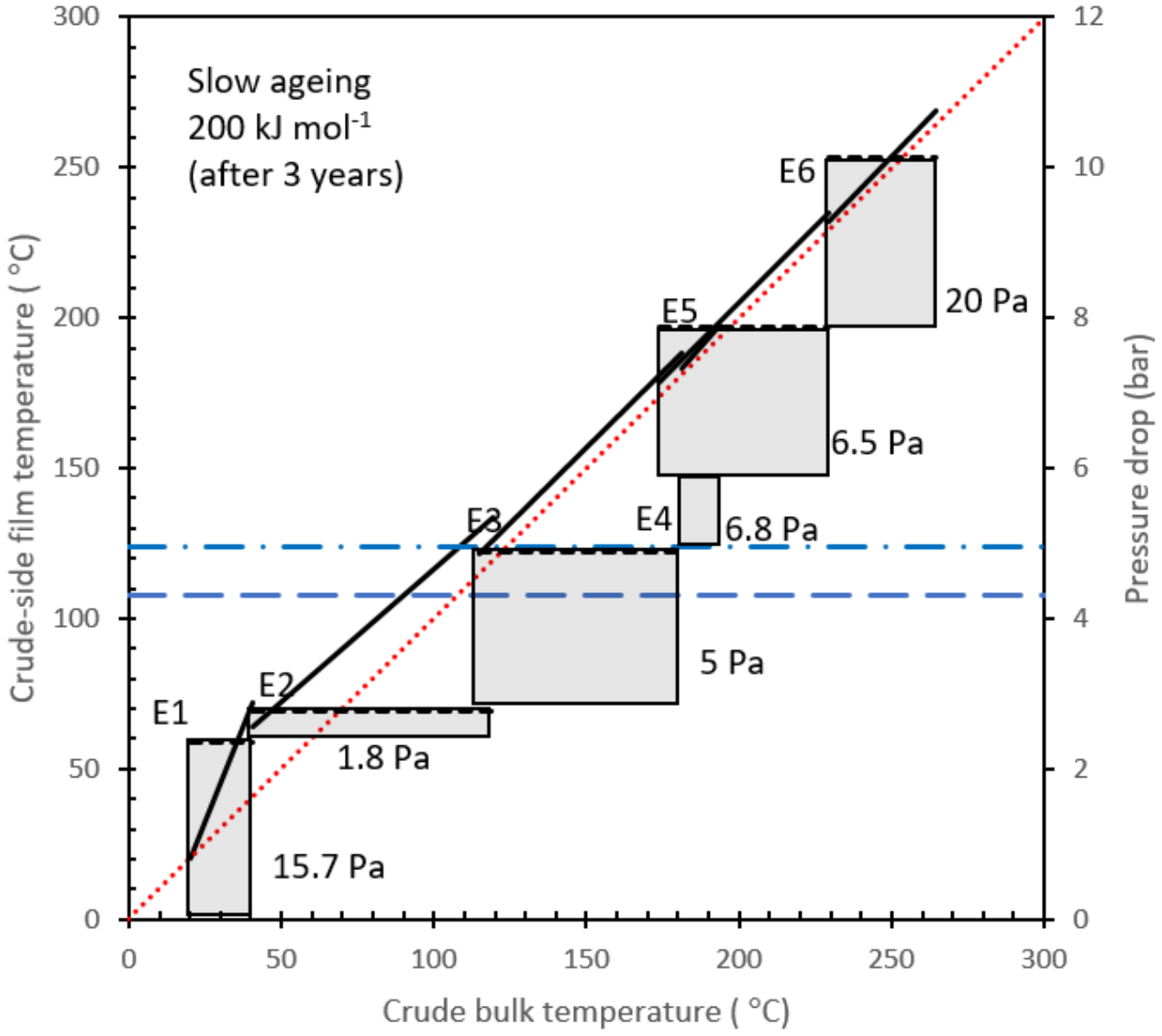

Figure 12. Modified temperature field plot for the Case Study network when after three years with (a) no ageing; (b) slow ageing, weak temperature dependency; (c) slow ageing, strong temperature dependency; (d) fast ageing, weak temperature dependency; (e) fast ageing, strong temperature dependency.

(e)

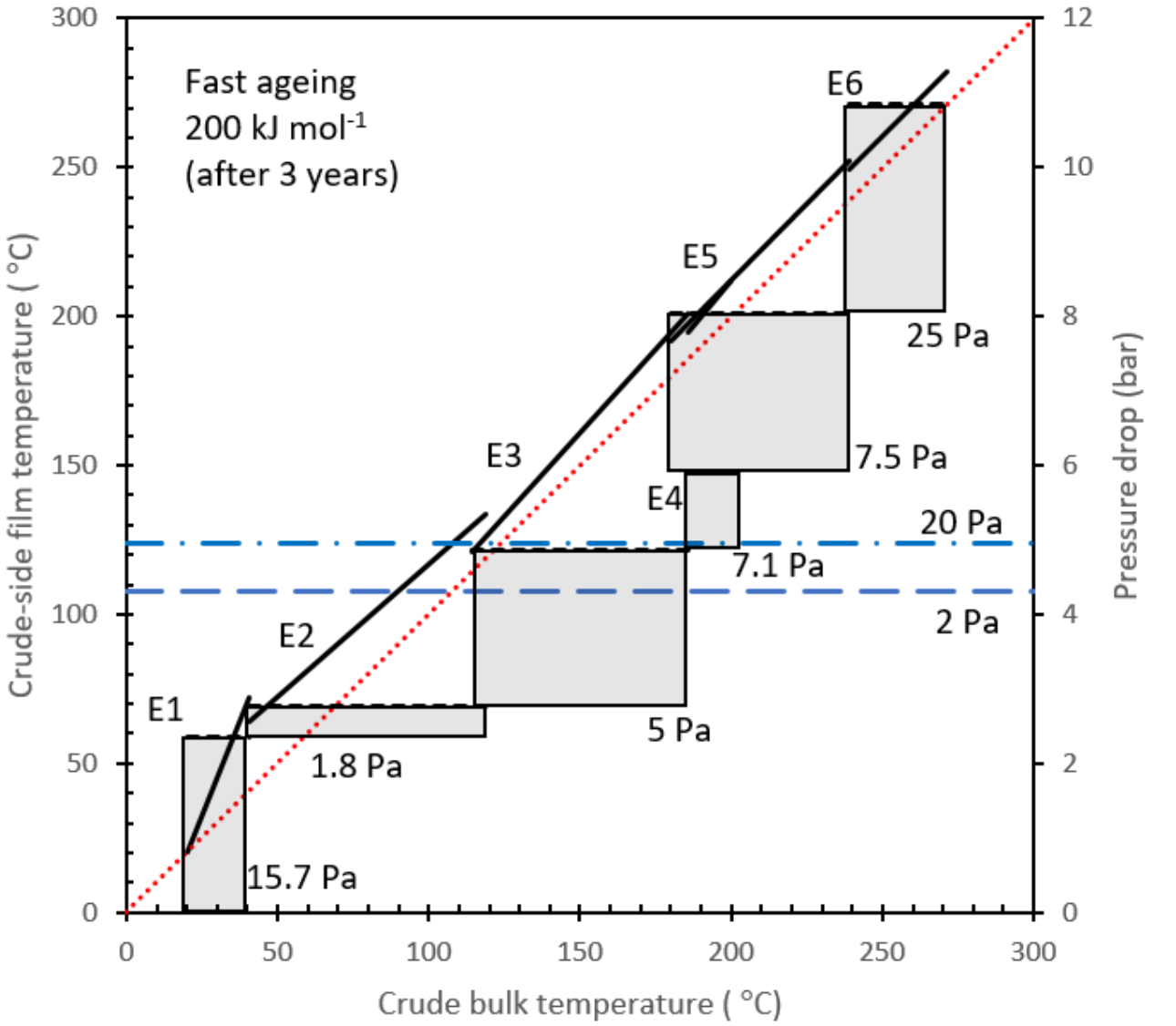

Figure 12. Modified temperature field plot for the Case Study network when after three years with (a) no ageing; (b) slow ageing, weak temperature dependency; (c) slow ageing, strong temperature dependency; (d) fast ageing, weak temperature dependency; (e) fast ageing, strong temperature dependency.